Evaluation of GFDL coupled climate models for western Arctic seasonal heat budgets

Marion Alberty*[1], Mary-Louise Timmermans[2], Sonya Legg[1], Robert Hallberg[3] - *corresponding author: malberty@princeton.edu

[1]Princeton University, [2]Yale University, [3]NOAA Geophysical Fluid Dynamics Laboratory

Introduction and Scientific Aim

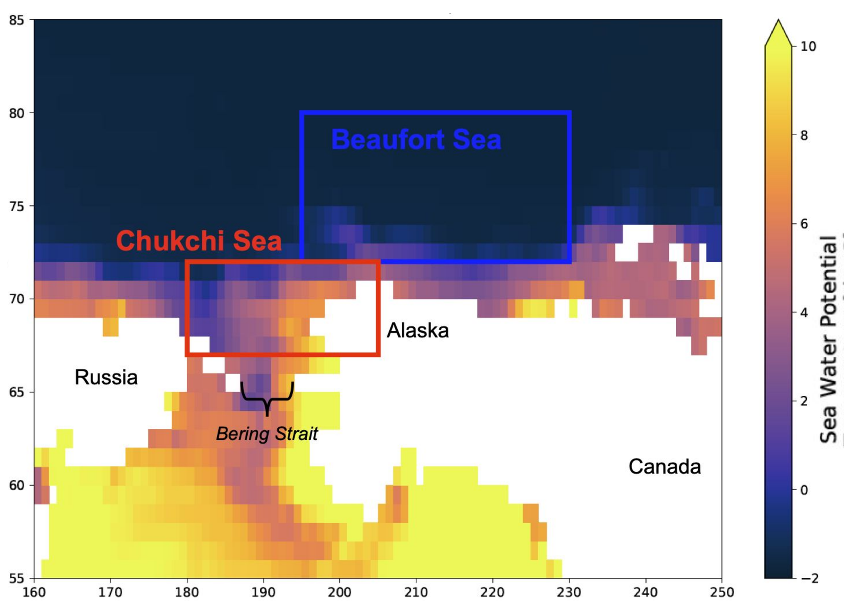

The Arctic is undergoing rapid change with atmospheric and oceanic warming, retreating sea ice, and shifting fish distributions. The greatest losses of sea ice have been in the Beaufort Sea and Chukchi Sea *(left, SST from CMIP6 CM4)* where approximately two thirds of the sea ice loss is attributed to ocean heat fluxes. *(Right)* Waters of North Pacific origin transport heat into the Arctic through Bering Strait (Q_{in}). Ocean heat content is modified over the Chukchi Sea ($Q_{Surface}$) and that warm, salty water is subducted under the mixed layer in the deep basin (Q_{out}), forming the warm halocline of the Beaufort Gyre. **While the Chukchi Sea plays a critical role in modulating the heat content of Pacific Water subducted into the Beaufort Gyre halocline on seasonal timescales, conflicting observational evidence leaves the Chukchi Sea's role in this heat transport unclear.**

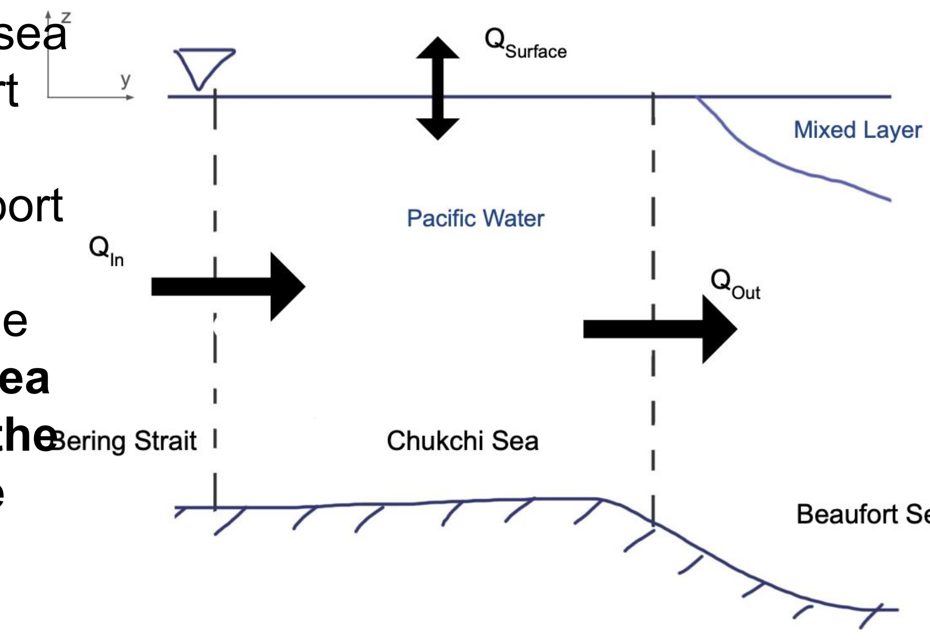

To address this uncertainty, a suite of ocean and coupled climate models produced at the National Oceanic and Atmospheric Administration Office's (NOAA) Geophysical Fluid Dynamics Laboratory (GFDL) are being utilized to close heat budgets for the Chukchi Sea. Here we present the evaluation of some of these simulations to quantify model biases and identify strengths, weakness, and uncertainties for the available configurations.

Model Data and Observations

Two configurations of the NOAA GFDL coupled climate model, CM4, are presented here. For both configurations, the ocean model uses the state-of-the-art MOM6 code with 75 vertical levels utilizing a hybrid vertical coordinate system (Adcroft et al, 2019). CMIP6 CM4 (Held et al., 2019) has a nominal horizontal grid spacing of 0.25°, while High Res (in development) has a spacing of 0.125°. The preindustrial control (PI) simulations are analyzed for both, and the historical simulation is also evaluated for CMIP6 CM4. Simulated ocean heat transport through Bering Strait is evaluated using mooring observations of temperature and ocean velocity at 66°N,169°W within Bering Strait from 1990-2020 (Woodgate, 2018). The evaluation uses the direct observations of water properties and the derived mooring transports and fluxes at monthly and annual timesteps. A consistent reference temperature of -1.9°C is used for the observational and model heat flux and transport estimates.

Simulated surface winds are compared with reanalysis outputs from the European Centre for Medium-Range Weather Forecast (ECMWF) ERA5 model (Hersbach et al., 2019). Monthly and seasonal climatologies are generated for all simulations and the ERA5 reanalysis from 1979 to 2014 is averaged and down-sampled to the model grids to calculate biases in the climatologies over the Pan-Arctic (lat > 60°N).

Q_{in}: Bering Strait Inflow

A key source of heat for the Beaufort Gyre is the Pacific origin waters transported through Bering Strait. The transport structure can be divided into a broad, background flow and a strong, narrow Alaskan Coastal Current (ACC) *(below, left)*. Simulations capture the relatively warm *(below, middle)* and fresh *(below, right)* properties of the ACC.

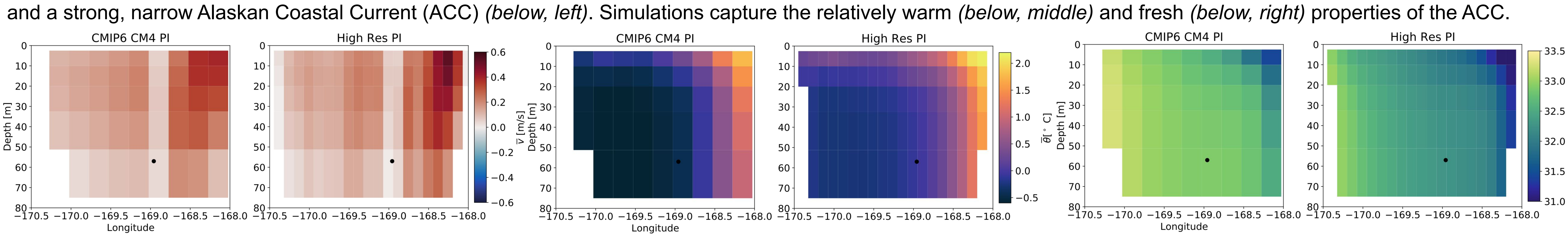

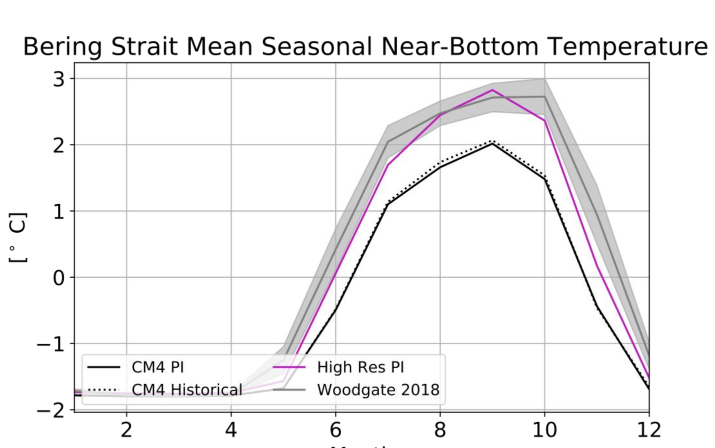

Comparison between the moored, near-bottom observations of temperature *(left)* and salinity *(right)* with the nearest grid point in the chosen simulations indicate an **improved agreement of both properties in the High Resolution simulations**. A similar comparison with near-bottom meridional velocities is limited by the presence of an island wake in the simulations. However simulated monthly mean volume transports through Bering Strait *(below, left)* are consistent with observational estimates, though monthly observations do not include a correction of ACC transports. This leads to agreement between the simulated and observed estimate of the monthly heat flux *(above, right)*, again with the caveat that monthly observations do not account for the ACC. The location of the mooring observation is noted with the black dot in the above colormap figures.

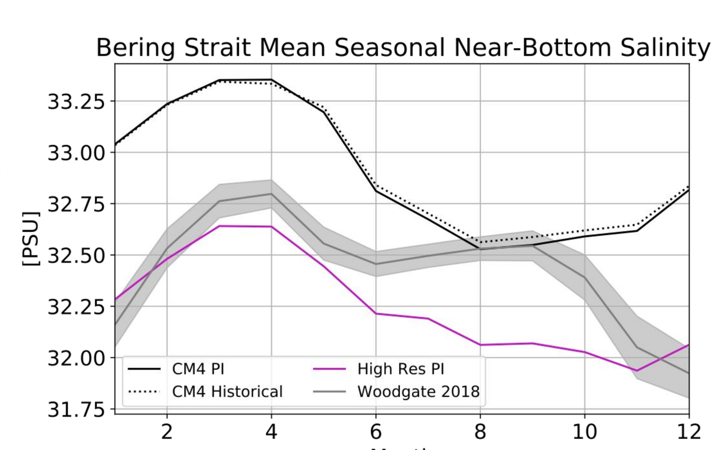

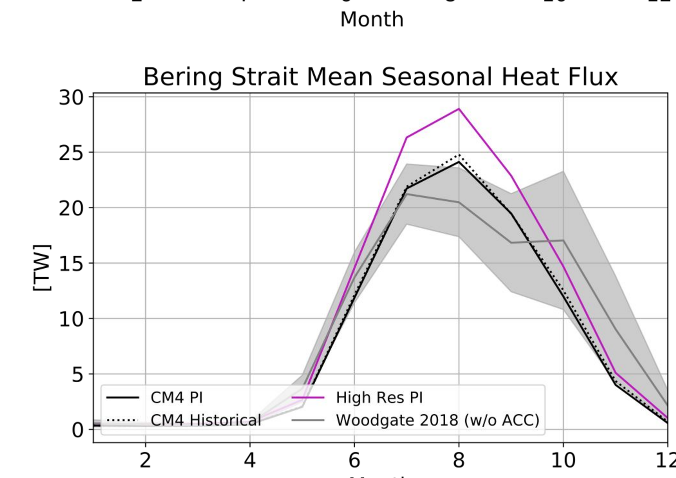

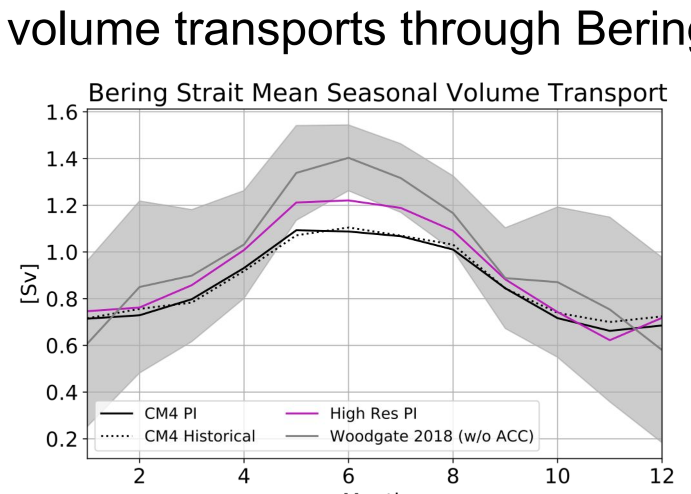

Annual mean volume transport (T_{vol}) and total heat transport (T_{heat}) for all three simulations are less than the observational estimates (which do include a correction for the ACC transport) (Table below).

	Woodgate 2018	CMIP6 CM4 PI	CMIP6 CM4 Hist	High Res PI
T_{vol} [Sv]	1.07 ± 0.12	0.86 ± 0.06	0.87 ± 0.07	0.92 ± 0.08
$\sum T_{heat}$ [10^{20} J]	4.38 ± 1.20	2.57 ± 0.40	2.63 ± 0.45	3.13 ± 0.48

While all simulation estimates are low relative to the observations, the High Res PI simulation is in closest agreement with the mooring estimate. The mooring estimate of both quantities also demonstrates a strong positive trend since the year 2000 *(below for T_{heat})* and thus the observational estimate is likely an upper bound for any preindustrial estimate. A key feature missing in CM4 Historical is the rapid increase in both T_{vol} and T_{heat} since 2000 which will be a source of uncertainty in present-day budget estimates.

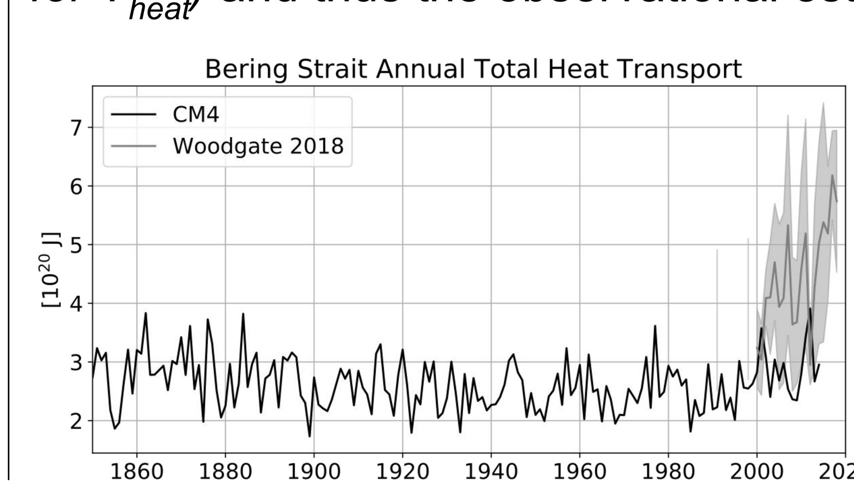

$Q_{Surface}$: Surface Winds

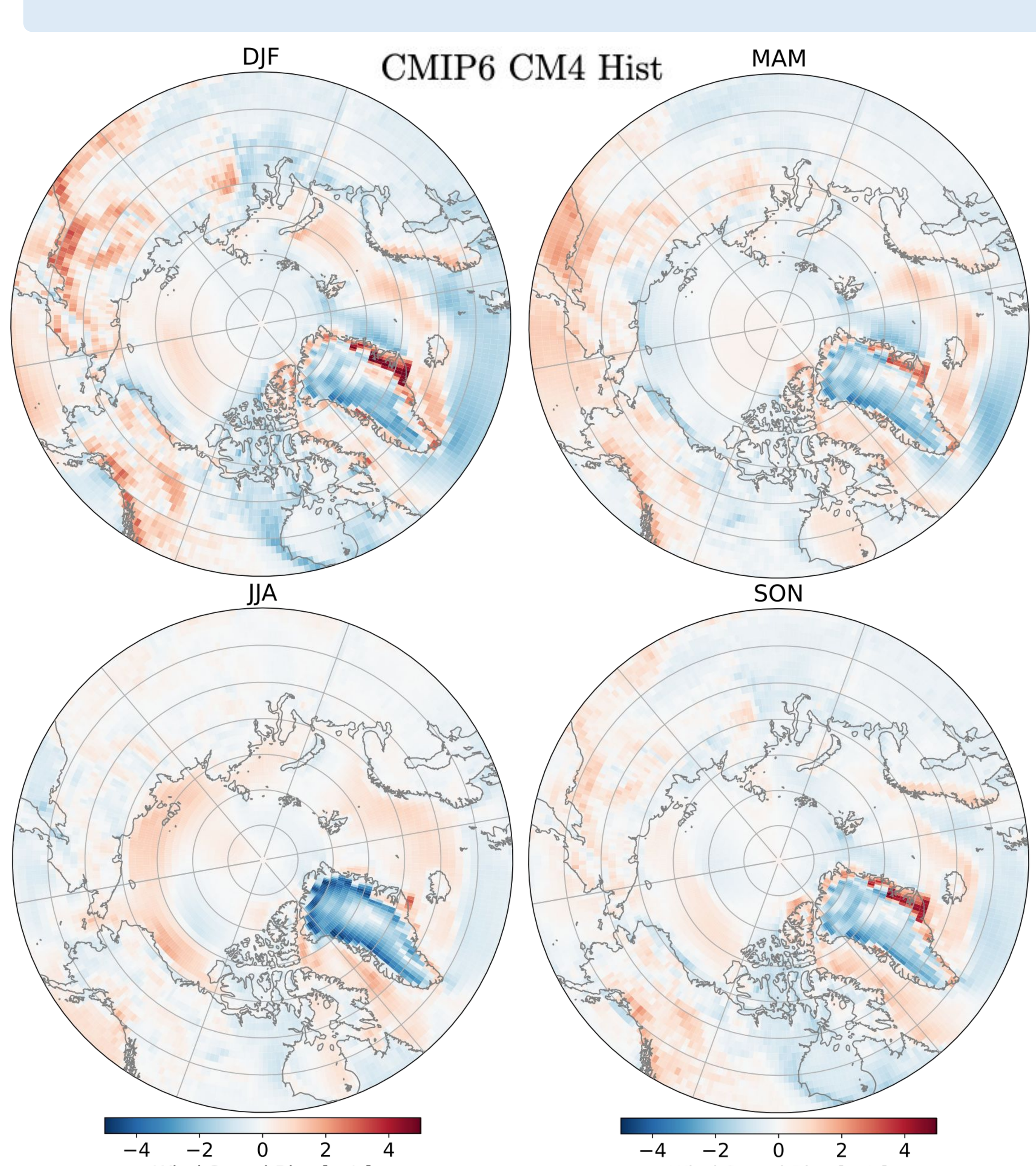

Biases in the simulated seasonal wind fields have strong spatial variability over the Arctic with the largest biases concentrated around Greenland *(left)*. On average, Pan-Arctic biases are largest in winter for all three simulations *(right)*, indicating relatively weak winds, and thus air-sea fluxes for that season. Restricting the bias estimate to the Chukchi and Beaufort Seas (far right), produces similar results, with relatively weak winds from December to April in the preindustrial control simulations. **For all three simulations, surface wind speed biases are weaker in summer when air-sea heat fluxes are strongest.** Additional evaluation of simulated and observed air-sea heat fluxes will be calculated, including the biases in climatological surface radiation, latent and sensible heat fluxes, and seasonal sea ice cover.

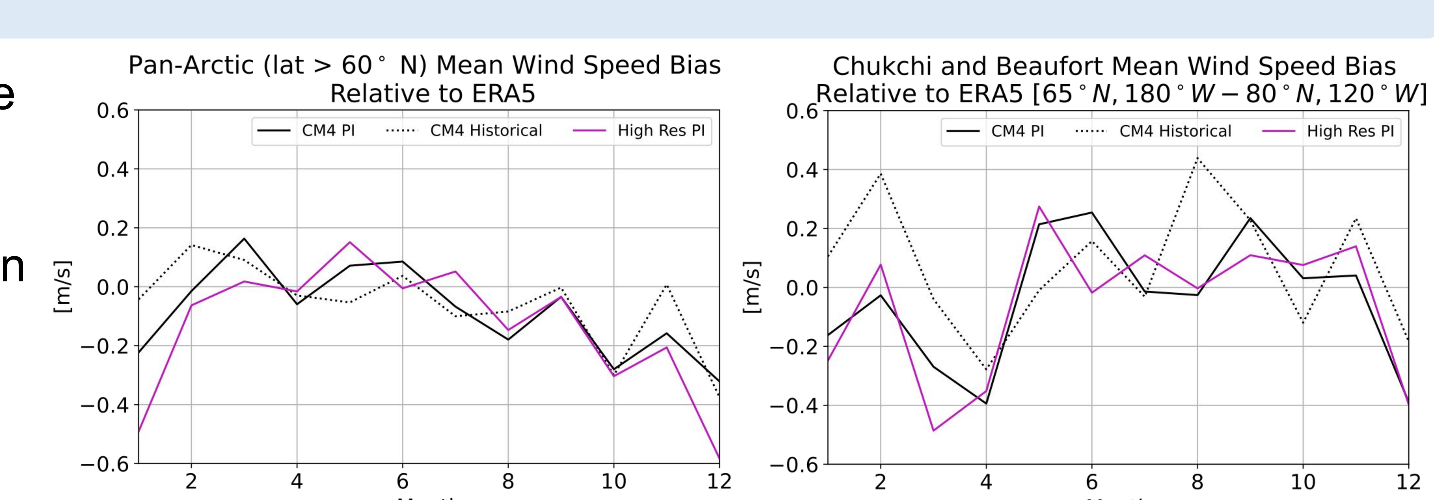

Future Work: Beaufort Gyre Heat Content and Water Properties

A remaining step is to evaluate the water properties and heat content of the Beaufort Gyre to provide context and error estimates in the calculation of Q_{Out}. Temperature, salinity and pressure observations from Ice-Tethered Profilers will be used to estimate the heat content within density layers in the Beaufort Gyre and compared with simulated heat content. The difference in layer-by-layer heat content will be used to determine if the simulations subduct a similar quantity of heat into the Beaufort Gyre halocline and how the simulations redistribute that heat relative to the observations.

Acknowledgements

This work was done while M. Alberty was supported by a NSF OCE PRFP. We thank the many scientists and engineers at NOAA GFDL for the model data. Mooring data is detailed in Woodgate, 2018. Hersbach et al., 2019 was downloaded from the Copernicus Climate Change Service (C3S) Climate Data Store.